

Modularized and scalable compilation for quantum program in double quantum dots

Run-Hong He¹, Xu-Sheng Xu^{2*}, Mark S. Byrd³ and Zhao-Ming Wang^{1†}

1. *College of Physics and Optoelectronic Engineering,
Ocean University of China, Qingdao 266100, China*

2. *Department of Physics, State Key Laboratory of Low-Dimensional Quantum Physics,
Tsinghua University, Beijing 100084, China and*

3. *Department of Physics, Southern Illinois University, Carbondale, Illinois 62901-4401, USA*

Any quantum program requires compiling into an executable form according to the underlying hardware characteristics. While the stringent restrictions on control imposed by certain physical platforms may make this task challenging. In this paper, based on the quantum variational algorithm, we propose an novel scheme to train the Ansatz circuit and exemplarily realize high-fidelity compilation of a series of universal quantum gates for singlet-triplet qubits in semiconductor double quantum dots, a typical heavily constrained system. Furthermore, we propose a scalable architecture to modularly implement quantum programs in this constrained systems and validate its performance with two representative and meaningful demonstrations, i.e., the Grover's algorithm for the database searching (static compilation) and a variant of variational quantum eigensolver for the Max-Cut optimization (dynamic compilation). Our work constitutes an important stepping-stone for exploiting the potential of this physical resource for advanced and complicated quantum algorithms.

Benefiting from the specific properties of superposition and entanglement, the quantum computers often admit superpolynomial or even exponential acceleration over their classical counterparts in solving certain important and intractable problems [1, 2]. In the race to construct quantum computing prototypes, a wide range of physical models have been proposed and experimentally demonstrated over the past decades, including trapped ions [3], ultracold atoms [4], nitrogen-vacancy centers [5], superconducting circuits [6–9], optical system [10, 11] and semiconductor quantum dots [12, 13], etc. Particularly, the semiconductor quantum dots is favored as a promising competitor, notable for researchers owing to the long-lived coherence of spins in solid-state systems, prospective scalability and compatibility with existing mature semiconductor manufacturing techniques [14–17]. By leveraging the degrees of spin and charge of electrons trapped in quantum dots, various qubit modalities have been suggested and realized in experiments, such as the single-electron spin-1/2 qubit [16], two-electron singlet-triplet (S - T_0) qubit in double quantum dots (DQDs) [18–21], three-electron exchange-only qubit [22, 23] and hybrid qubit [24, 25]. Among them, the S - T_0 qubit has attracted considerable interest because it can be manipulated all electrically and provides rapid gates in sub-nanosecond time scales, which is fast enough to enable 10^4 gates before the decoherence falls [26].

Any high-level algorithm for quantum computation needs translating into low-level instructions that can be executed step by step on specific quantum hardware [27–30]. While the S - T_0 qubit is one of the most promising modalities towards a scalable quantum computer from

the fabrication perspective, the tight restrictions on the control precludes the applications of many existing optimization methods and make it uniquely challenging to manipulate this quantum system for computational tasks on demand [31, 32]. The primary hurdles arise in physical details that **1)** one could only precisely control the rotation rate around the $+z$ -axis of a single-qubit state on the Bloch sphere, while the rotation rate around the x -axis is constant and non-zero; **2)** the undesired coupling introduced by simultaneous operations on adjacent qubits would fail these intended individual operations.

To date, enormous ingenuities and efforts have been devoted to compiling required operations into sequential native gates on this platform, such as the so-called SUPCODE [32–34] for generating robust quantum gates and fast geometric gates [35] for cancelling out the accompanied dynamical phase during evolution. A native gate in this paper refers to an operation that can be readily implemented in DQDs with a single (for single-qubit operation) or pair (for two-qubit operation) of pulses. Typically, for performing arbitrary rotation gates, it is necessary to solve iteratively a set of nonlinear equations and therefore determine the appropriate composite pulse sequence [32, 36]. Thus it is an resource-expensive and time-demanding task in practice. Aimed at improving the efficiency of tailoring pulse sequence, a significant surge of interest recently is focused on nascent tools. For examples, by employing the machine learning [37], Ref. [36] studies how to predict directly the required pulse sequence with a well-trained neural network; Ref. [31] promises to steering dynamically a specific quantum state to another; Ref. [38, 39] could reset arbitrary quantum state to a target one, and contrastively Ref. [40] shows the capability of arbitrary quantum state preparation from $|0\rangle$. Furthermore, high fidelity universal quantum state preparation is also

*thuxxs@163.com

†wangzhaoming@ouc.edu.cn

observed in [41] with the revised greedy algorithm. All of them exhibit excellent performance in universal gates construction or few-qubit state preparation, whereas the lack of an architecture that can properly combine together these pulse sequences of varying lengths makes it hard to perform practical computation due to the aforementioned second limitation in DQDs - an unfinished operation on one qubit will interfere with the execution of quantum gates on its neighboring qubits, thus resulting in the absence of scalability. An open problem and important direction of investigation for this special system is therefore to develop a compiling architecture which could layout varied native gates scalably for impactful computational tasks. Available traditional optimization approaches that could yield fixed-length pulse sequence are mainly based on the gradient, such as the stochastic gradient descent [42]. Partly due to the fact that each gradient evaluation requires two forward passes for loss function calculation, their resource consumption grows very quickly as the size of parameter space increases. In addition, their performance are sensitive to the random initialization, and as a consequence the optimization often be stucked in a local optimum and then quits with an inadequate fidelity.

In this paper, we enlist another emerging and powerful technique to compile the desired unitary into native gate sequence with unchanged length - the variational quantum algorithm (VQA) [43, 44], which has recently been used for decomposing complex unitary into ordered universal gates [45, 46] or Schmidt decomposition [47], etc. Utilizing the adjoint differentiation [43, 48], the VQA permits gradients collection of all parameters with only one forward pass and one recursive backward pass [43] - a tempting calculation saving compared to traditional gradient-based methods. Additionally, we suggest training the Ansatz, a circuit of parametric native gates, with random quantum states. Compared to the widely used matrix-based approaches [45–47], this training scheme offers reduced overhead in loss calculation and smaller possibility of being stucked in local optimums during optimization. Considering single-qubit rotations and entangling two-qubit gates are crucial ingredients for universal quantum computation, a series of them are exemplarily compiled and high fidelities are reached, underling the foundations for performing precisely quantum programs in DQDs.

More importantly, inspired by the special stacking style of Mahjong cards, a traditional Chinese chess game (see Fig. 4(a)), we present a modularized and scalable (MS) compilation architecture that can systematically combine native gate sequences served as logic operations to perform advanced and complex reference quantum circuit in DQDs. Finally, we demonstrate our MS compilation with two representative quantum computing tasks, i.e., the Grover’s algorithm [49–51] for database search and a variant [52] of variational quantum eigensolver (VQE) [53–56] for

graph Max-Cut optimization [57], and achieve incredible results. These results show that our MS compilation can be a powerful tool used to exploit the potential of DQDs in current noisy intermediate-scale quantum era [58].

Results

Model

In the present work, the model of interest is the semiconductor DQDs system, where the S - T_0 qubit is encoded in the collective spin states of two electrons confined in a double-well potential [26, 59]. The Hamiltonian of a single S - T_0 qubit governed by external electric pulses reads [12, 13, 19, 60]

$$H(t) = J(t)\sigma_z + h\sigma_x, \quad (1)$$

under the computational basis $\{|0\rangle = |S\rangle = (|\uparrow\downarrow\rangle - |\downarrow\uparrow\rangle)/\sqrt{2}, |1\rangle = |T_0\rangle = (|\uparrow\downarrow\rangle + |\downarrow\uparrow\rangle)/\sqrt{2}\}$. σ_z and σ_x are Pauli matrices and result in the rotations of the quantum state around the z - and x -axes with rates $J(t)$ and h , respectively. The coefficient h indicates the Zeeman energy splitting between $|S\rangle$ and $|T_0\rangle$, commonly raised by nearby deposited permanent micromagnet [60] and its value is difficult to vary during the quantum gate time in experiment [59, 60] (although tunable splitting stemmed by Overhauser field has been observed [26], its time consumption is much longer than a typical gate time). We assume $h = 1$ here to facilitate our theoretical treatment, and take it as the energy unit. The only effective tunable parameter in this system is the exchange coupling $J(t)$ between two captured electrons and can be rapidly manipulated by applying calibrated voltage pulses to the associated electrodes. In addition, for simplicity, the reduced Planck constant is also held $\hbar = 1$ and served as the time-scale throughout. Because of the nature of exchange interaction and to avoid altering the charge configuration of the quantum dots, $J(t)$ is constrained to be non-negative and bounded, i.e., $J_{\max} \geq J(t) \geq 0$, where the maximal value $J_{\max} \sim h$ [33]. In other words, we have only precise control over the rotation rate of the quantum state around the $+z$ -axis on Bloch sphere, while the rotation rate around the x -axis is always present and invariable.

Experimental available native gate (one-piece rotation) can be realized by applying electrical pulse with specific intensity J for a certain amount of time Δt , which produces a rotation around the axis $J\vec{z} + \vec{x}$:

$$g(J, \Delta t) = \exp(-i(J\sigma_z + \sigma_x)\Delta t). \quad (2)$$

A special case is that if we set $J = 0$, then $g(0, \Delta t) = \cos(\Delta t) \cdot I + i\sin(\Delta t) \cdot \sigma_x$, where I refers to the identity operator. In this case, the identity gate g_I can be achieved, up to an irrelevant global phase, when $\Delta t = k\pi$, where k are integers. This point will prove invaluable and plays the role of a major groundstone for our MS compiling architecture in DQDs as we will discuss in **Methods**.

In order to generate entanglement between qubits, multi-qubit entangling gates are necessary. In DQDs,

the effective Hamiltonian of two adjacent qubits based on Coulomb interaction can be written as [13, 61, 62]

$$H_{2\text{-qubit}} = \frac{\hbar}{2}(J_1(\sigma_z \otimes I) + J_2(I \otimes \sigma_z) + h_1(\sigma_x \otimes I) + h_2(I \otimes \sigma_x) + \frac{J_{12}}{2}((\sigma_z - I) \otimes (\sigma_z - I))), \quad (3)$$

under the basis of $\{|SS\rangle, |ST_0\rangle, |T_0S\rangle, |T_0T_0\rangle\}$. J_i and h_i are exchange interaction and Zeeman splitting respectively, with the subscript $i = 1, 2$ referring to the corresponding qubit. Empirically, the inter-qubit coupling $J_{12} \propto J_1 J_2$ [61] and here we assume $J_{12} = J_1 J_2 / 2$ again for simplicity. As in the case of single S - T_0 qubit, the operation on this two-qubit system requires only pulsed electric fields, i.e., J_1 and J_2 . To maintain the coupling between two qubits, it has to keep $J_i > 0$ during entangling operations. It is important to notice that the coupling term in Eq. (3) also informs us that to manipulate a certain qubit individually, we have to suspend the control on its neighboring qubits to avoid undesired inter-qubit coupling. These restrictions should be kept in mind all the time when we design the architecture to run quantum program.

Compilation for universal gates

Considering the necessity of universal quantum gates for the implementation of quantum programs [1, 2], in this subsection, we first study the applicability of the MS compilation in arbitrary single-qubit gates and then move attention to exploring common two-qubit entangling quantum gates. The details of the gate compiling process are shown in **Methods**. We stress that, for conciseness, the control pulses are assumed to be piecewise-constant that are turned on and off instantaneously. In real experiments, pulses possessing finite rise times will result in only a minimally alteration in pulse parameters yield by our work but does not fail the major conclusion, as clearly explained in Ref [33], thus leaving it an justified assumption.

We use the Ansatz circuit to approximate the reference gate, hence its structure is crucial to the final result. The performance of the Ansatz for same 32 random reference quantum gates versus the number of employed native gates is plotted in Fig. 1, whose caption captures the detail information, such as pulse duration and learning rate. Fig. 1(a) describes the distribution of Ansatzs' final errors compared to the associated reference quantum gates vary with the number of native gates, where the black dashed line is a predefined error threshold, $1E-5$. When the validating error ϵ reaches this expected threshold (compiling succeed) or the number of training exceeds 4000 (compiling failed), the optimization ends.

From the evaluation results on sampled reference gates showed in Fig. 1(a), we can learn that once the native gate count below 10, there always exist points that cannot reach the error threshold, and this phenomenon is originated from that the limited Ansatz

space contributed by not enough native gates cannot cover the intended reference unitary. Although two bad points (which overlap because of similar error) are present when the native gate number is 11, they can also achieve the error requirement after 630 and 292 times of training respectively by changing the learning rate from 0.05 to 0.1. When the involved native gate count reaches 12 or more, arbitrary single-qubit operations can be implemented with a fair amount of confidence. Considering more native gates would impose additional overhead for optimization and experimental implementation, we believe that an Ansatz composed by 12 native gates is a beneficial trade-off between approximate precision and computational overhead for arbitrary single-qubit operation in our discussion.

This argument is also supported by Fig. 1(b), which depicts the averaged number of training for reaching the termination condition of optimization in terms of the applied native gate count. The required number of training gradually drops as the native gate count increases, implying that a deeper Ansatz circuit is more adequate for approximating the reference unitary. And this trend has been well maintained until the native gate count reaches 12. We emphasize that the above results are obtained under the assumption that the duration of the native gate is $\pi/2$. Other settings may deliver different results, but the final conclusion will be similar.

Non-parametric universal quantum gates are necessary for the quantum algorithm implementations. For example, Hadamard transformations composed of H gates are indispensable in the Grover's search algorithm, and X gates are also required in VQE to generate the Hartree-Fock initial states [55, 64]. Table I lists a series of common single- and two-qubit non-parametric quantum gates realized in the context of DQDs according to the MS compilation. We note, these solutions can be further used in different works, just as what we will demonstrate in the forthcoming subsection. After the optimization, all of the Ansatz achieve the specified error, $1E-5$, compared to the associated reference gates. All parameters are initialized to 1 before training and kept in the non-negative domain during the optimization to account for the experimental limitation. The Ansatz used for realizing single-qubit gates employ 12 single-qubit native gates with $\pi/2$ duration. The form of the Ansatz for two-qubit gate is that as depicted in Fig. 4(b) in Methods with pulse duration $\pi/10$ for single-qubit native gates and $\pi/2$ for two-qubit native gates, making a total of 6π runtime. So that it can work in synergy with Ansatz with the same runtime for arbitrary single-qubit gate. The corresponding learning rate and number of training used in optimization is collected in the second and third lines, respectively. More detailed information, e.g., the final pulse strengths, can be found in our online repository [65] in Gitee. In general, the design of two-qubit gates is more challenging than the single-qubit operations, as revealed by the fact that the former requires prudently selected learning rate and

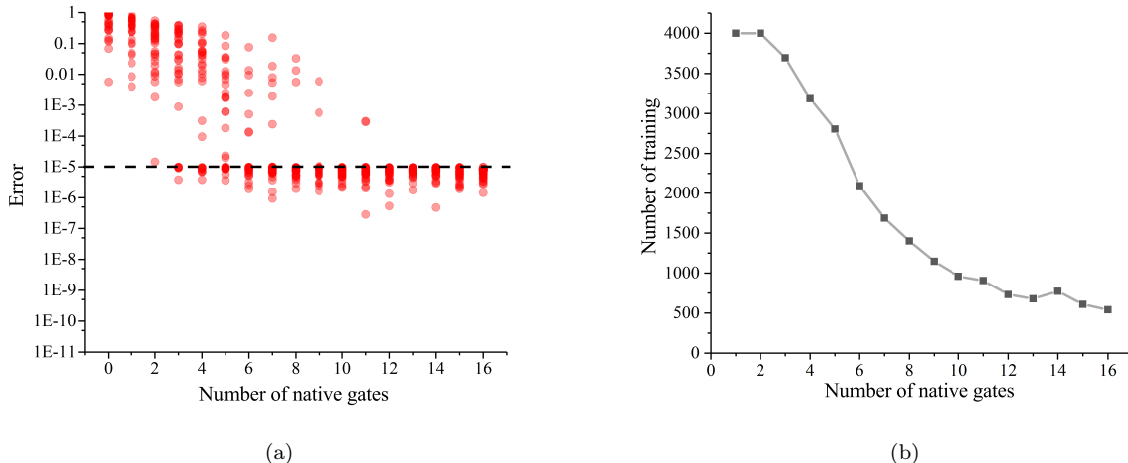


FIG. 1: The performance of the Ansatz for 32 single-qubit random reference unitaries vary with the number of employed native gates. (a) The distributions of the final errors run over the validating set with 100 random quantum states. The optimization ends when the error reaches the expected threshold (the dash line) or the number of training exceeds 4000. (b) The required averaged number to end the optimization as function of the number of native gates involved in the Ansatz. The duration of the native gate is $\pi/2$ and the optimizer used here is the Adam [63] with learning rate 0.05. All parameters are ones initialized before training and are kept in the non-negative domain during the optimization for respecting the experimental limitation.

much more times of optimization.

TABLE I: A series of common non-parametric universal quantum gate has been realized with MS compilation in DQDs. After the number of training captured in the third line, their validating errors relative to the associated reference gate all below the threshold $1E-5$. Every single-qubit logical gate are brought about by 12 single-qubit native gates with duration $\pi/2$. The structure of the Ansatz for two-qubit gates is depicted in Fig. 4(b) in Methods with pulse duration $\pi/10$ for single-qubit native gates and $\pi/2$ for two-qubit native gates. All parameters are initialized to 1 before training. The learning rate for optimization is captured in the second lines.

	H	T	S	X	Y	Z	CX	CZ
Learning rate	0.05	0.05	0.05	0.05	0.05	0.05	0.1	0.02
Number of training	676	552	871	412	594	600	3308	1162

Compilation for quantum programs

In this subsection, we validate the performance of our MS compilation with two demonstrations in DQDs: the Grover’s search algorithm [49–51] and graph Max-Cut optimization [57]. Our first demonstration aims to check whether the compiled circuit can faithfully execute the pre-designed and non-parametric reference circuit, i.e., static compilation [27]. While the second demonstration is to test if the MS compilation allows the DQDs native circuit to dynamically update its parameters efficiently to implement variational tasks, i.e., dynamic compilation [27].

We first focus on how to implement the Grover’s search algorithm in DQDs system by leveraging the MS compilation. For the problem of searching the target

items from an unordered database, the quantum Grover’s search algorithm permits a quadratic speedup compared to classical algorithms [1]. Here, we consider a two-qubit Grover’s search algorithm, where the presumed target state $|\omega\rangle = |11\rangle$. The reference circuit for this task is showed in Fig. 2 (a), which contains one Hadamard transformation and one Grover iteration carried out by the Oracle operator U_w and the Flip operator U_s . All of logical gates in this reference circuit are compiled by the MS compilation into a native gates sequence which consists of only DQDs. In addition, the forms and parameters of Ansatzs are directly copied from the results in the previous subsection and **Methods**. After execution, measurements are performed on the qubits and the probability distributions of the different results are shown in Fig. 2(b). From Fig. 2(b), we can learn that the correct result “11” can be obtained with near unit probability in measurement. This demonstrate that the QDQs systems with MS compilation can precisely execute pre-designed quantum programs.

The second demonstration for our MS compilation is to solve the graph Max-Cut optimization in DQDs system. The Max-Cut optimization is a typical NP-hard problem [66], which divides the vertices of an undirected graph into two parts and to maximize the sum of weighted edges being cut. For a graph with few vertices, its Max-Cut solution can be found within a reasonable amount of time by exhaustive enumeration. However, the classical algorithm will fail quickly because the resource overhead rises exponentially as the graph size scales up. Various of VQA were developed to provide the quantum advantage [67, 68] with contemporary noisy intermediate-scale quantum device, such as the quantum

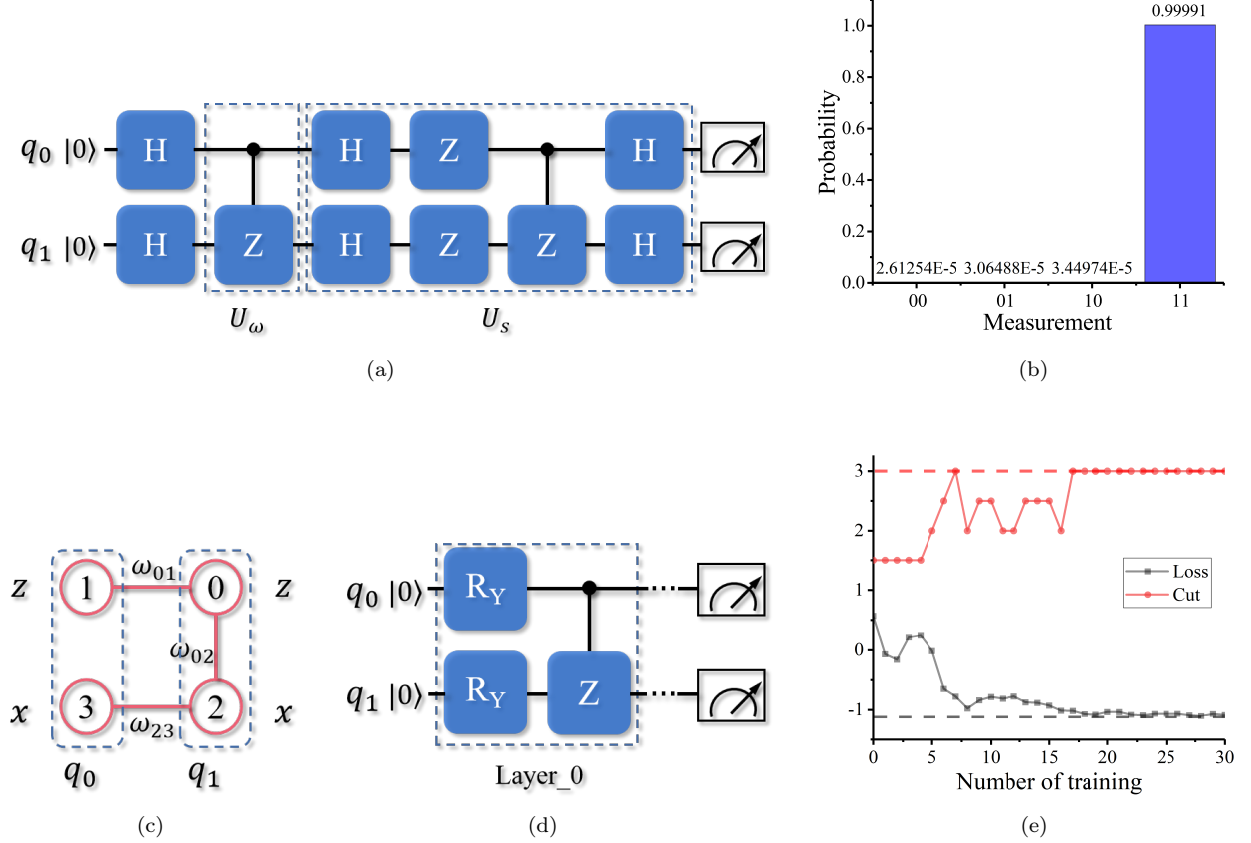


FIG. 2: Two demonstrations of MS compilation in two-qubit DQDs system: the Grover’s search algorithm and the MBE-VQE for graph Max-Cut optimization. (a) The reference circuit for Grover’s search algorithm with presumed target item “11”. This reference circuit will be compiled, according to the MS compilation, into circuit of native gates with fixed structure and parameters before execution. (b) Numerically calculated probability distributions of different measurements, yield by the compiled version of the reference circuit (a) in DQDs system with MS compilation. (c) An undirected graph with 4 vertices and 3 edges can be represented with a two-qubit system by MBE-VQE. (d) The reference circuit with multiple basic layers used to implement a two-qubit MBE-VQE for graph Max-Cut problem. (e) The predicted cut result and loss value as functions of number of training in DQDs with MBE-VQE and MS compilation for the Max-Cut optimization of graph (c). The red and black dashed lines are the final values of cut count and loss obtained by unrestricted system, respectively.

approximate optimization algorithm [69] (QAOA), which utilizes n qubits for the Max-Cut optimization of a graph with n vertices. By virtue of multi-basis graph encoding and nonlinear activation functions, based on traditional VQE [53–55, 64] and tensor network [70–72], the multi-basis encodings VQE (MBE-VQE) acquires improved performance with only half quantum hardware overhead (qubit number) as well as shallower quantum circuit, and admits quadratic reduction in measurement complexity compared to the traditional VQE [52].

For concreteness, we consider an undirected graph with 4 vertices and 3 edges (see Fig. 2(c) for a schematic representation). In MBE-VQE algorithm, this graph can be represented with a two-qubit system: for example, vertices 0 and 2 are encoded into qubit q_0 while vertices 1 and 3 into qubit q_1 . In addition, the vertices 0 and 1 are mapped to the z -axis while the vertices 2 and 3

to the x -axis as showed in Fig. 2(c). The loss function is made up with products of single-qubit measurements $\langle \sigma_i^z \rangle$ and $\langle \sigma_i^x \rangle$, which are dressed by function $\tanh(x)$ and edge-weight ω_{ij} :

$$\begin{aligned} Loss = & \omega_{01} \tanh(\langle \sigma_0^z \rangle) \tanh(\langle \sigma_1^z \rangle) \\ & + \omega_{02} \tanh(\langle \sigma_0^z \rangle) \tanh(\langle \sigma_0^x \rangle) \\ & + \omega_{23} \tanh(\langle \sigma_0^x \rangle) \tanh(\langle \sigma_1^x \rangle). \end{aligned} \quad (4)$$

The Ansatz circuit in this task contains two basic layers composed of single-qubit rotation gates R_Y and entangling two-qubit gate CZ , as illustrated in Fig. 2(d). Each rotation operation R_Y is completed by 12 native gates with variable parameters and $\pi/2$ duration. While the structure and parameters for the CZ gates are directly adopted from the results obtained in the previous subsection. According to the MBE-VQE algorithm, the

predicted cut count is defined as

$$\begin{aligned}
 Cut = & \frac{\omega_{01}}{2} [1 - R(\langle \sigma_0^z \rangle) R(\langle \sigma_1^z \rangle)] \\
 & + \frac{\omega_{02}}{2} [1 - R(\langle \sigma_0^z \rangle) R(\langle \sigma_0^x \rangle)] \\
 & + \frac{\omega_{23}}{2} [1 - R(\langle \sigma_0^x \rangle) R(\langle \sigma_1^x \rangle)],
 \end{aligned} \tag{5}$$

where $R(x)$ denotes the classically rounding procedure.

For simplicity, we assume the weights of all the edges $\omega_{ij} = 1$. In this case, the correct solution of this Max-Cut problem is 3. Fig. 2(e) displays the loss value $Loss$ and predicted cut count Cut as functions of number of training, where the learning rate is set be 0.1 and all native gate parameters are ones initialized. The red and black dashed lines refer to the final values of Cut and $Loss$ yielded by unrestricted system, respectively. It can be clearly learned from Fig. 2(e) that the results of variational native circuit compiled dynamically by the MS compilation, after about 18 times of training, has almost no difference in both the predicted cut count and loss value compared to ideal results obtained in unconstrained system. This reveals that the DQDs system empowered by our MS compilation possess the potential to allow applications of variational algorithms.

We accomplish these simulations with MindQuantum [73], a nascent and fast-expanding high-performance software package for quantum computation. It allows efficient problems solving in quantum machine learning, chemistry simulation, and optimization. All detailed code and data that support this work are available in our online repository [65] for interested readers.

Discussion

For portability, quantum algorithms are generally programmed hardware-independent, which necessitates the effective compilation platform-specifically for practical implementation. Due to the severe and special constraints in DQDs, what should be kept in mind during design the compilation architecture is not only the high fidelity quantum gates compilation but also the approach which could combine them together appropriately to prevent undesirable inter-qubit coupling.

In this work, we suggested the usage of random quantum states in training the Ansatz in VQA for compiling or decomposing unitary to reduce resource overhead in loss calculation and to avoid the optimization being stuck in local optimums. The performance of Ansatz consisting of various numbers of DQDs native gates to achieve single-qubit rotations was explored and the proper trade-off was found. And then, a series of common non-parametric universal quantum gates had been exemplarily compiled and fair high fidelities were observed. Most importantly, we emphasized the necessity of constant-runtime quantum gates for the scalability and set up a scalable architecture, the MS compilation, which is able to layout the modularized native gates served as logical operations to avoid unwanted coupling

between surrounding qubits, and thus enable the faithful execution of the reference quantum circuit. Finally, to get an estimation of the performance, we presented two representative applications, the Grover’s search algorithm for static compilation and the Max-Cut optimization for dynamic compilation. Both deliver superb results, demonstrating its feasibility for realistic implementation in the experiments.

We believe these advances would be immensely helpful in exploiting the potential of DQDs system for performing complex and meaningful quantum programs, thereby reaching a further milestone in the path towards a practical large-scale general quantum computer.

Methods

In the section **Model**, we presented a typical restricted system, $S-T_0$ qubits in DQDs and pointed out where the difficulty of gate compiling lies. In this section, we start by explaining how to compile single-qubit arbitrary gate into sequential DQDs native gates by VQA and next describe an architecture that orchestrates operations on neighbor qubits to avoid unexpected interaction effects. Finally, a structure that enables two-qubit entangling gates is presented. With these elements, advanced quantum programs and algorithms can be performed in DQDs.

In our work, any reference unitary U_{ref} is compiled into DQDs native gates by leveraging the VQA. Taking the complication of an arbitrary single-qubit gate as an example, the overall workflow is schematically outlined in Fig. 3(a), where the Ansatz is composed of n native gates, denoted as blue blocks with subscript indicating which qubit is acted on. Each native gate is generated by an electric pulse with a certain strength J and duration. The process of achieving an appropriate native gates sequence that equivalent to the U_{ref} goes as follows:

Step 1: Ansatz’s variational parameters (J s) are all ones initialized before optimization and additionally restricted to the non-negative domain throughout the training process, accounting for realistic physical limitation of non-negative pulses strength as introduced in the previous sections.

Step 2: Certain amount of random quantum states are generated using quantum circuit containing random parameters, and divided into train and validation sets proportionally. The single- and two-qubit quantum circuit generating random states in this work are shown in Fig. 3(b) and (c), whose outputs can theoretically cover the entire Hilbert space as the real-valued parameters vary [74, 75].

Step 3: A random quantum state $|\phi\rangle$ sampled from the train set will: **1)** be fed to the Ansatz which then outputs the final state $|\varphi\rangle$ after evolution; and **2)** be acted by the U_{ref} and converted to the target state $|\psi\rangle$.

Step 4: Compute the loss function $Loss = -|\langle \psi | \varphi \rangle|^2$, which quantifies the fit of the effect of Ansatz to the U_{ref} . With the $Loss$ available, the gradient with respect to each Ansatz’s parameter can be calculated [43, 76–78]

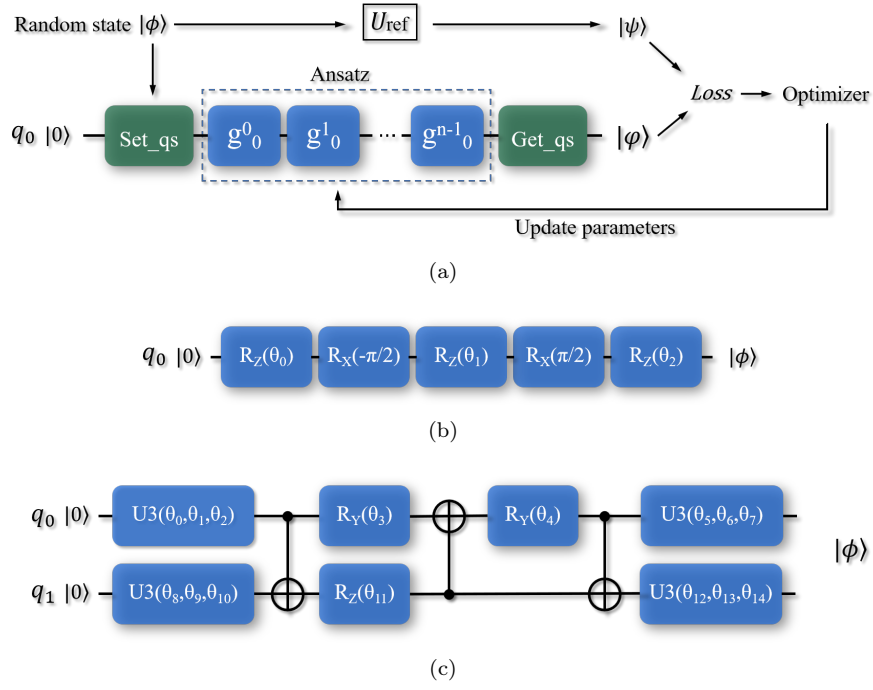


FIG. 3: (a) The overall workflow of the compilation of a reference logical single-qubit unitary U_{ref} with an Ansatz consisting of sequential native gates. Each native gate, denoted as a blue block, is carried out by a single electric pulse J with a certain duration acted on the DQDs qubit. The details of this workflow is described in text. (b) The so-called U3 circuit [73, 74] used to generate single-qubit random quantum states for training one-qubit Ansatz. (c) The parametric circuit [75] used to generate two-qubit random quantum states for training two-qubit Ansatz.

and then used to update the parameters for improving the performance by an optimizer, such as the Adam [63, 79].

Step 5: Validate all random states in validation set using the process similar to the step 3 and then take the smallest $1 + \text{Loss}$ among them as the current error ϵ of the Ansatz relative to the reference unitary at this train step.

Repeat the sequential steps 3-5 until the error ϵ over the validation set smaller than an acceptability threshold, such as $1\text{E-}5$, where the effect of the Ansatz will be well equivalent to the target U_{ref} .

Compared to schemes [45–47] who update the Ansatz’s parameters in a closed-loop style, the application of random state reduces the susceptibility of the optimization to local optimas, akin to the usage of random samples in the training landscape of classical neural networks [38]. In addition, the utilization of quantum states are more resource efficient than commonly used approaches based on matrices in loss calculation, such as the Hilbert-Schmidt distance or other customized metrics between the associated unitary [45–47]. It is worth noting that this training approach is scalable and applicable generally to the construction or decomposition of unitary with any qubit count.

As for the implementation of individual operations on different qubits, the challenge raises from the fact that if the pulses imposed on adjacent qubits are non-zero

simultaneously, these qubits will interact with each other due to capacitive coupling [13], and therefore precludes the access of intended manipulations. Inspired by the Mahjong (shown in Fig. 4(a)) whose cards are stacked upright so that no interaction produces between adjacent columns and thereby they can be operated independently, we propose the following architecture to circumvent this intractable problem.

We make the execution time of all Ansatzs for the associated logical gates to be the same (constant pulse sequence length), and when a certain qubit is operated on, its neighboring qubits are set to be idle (no pulses acting on), so as to avoid interferences between qubits. While the idle qubits undergo free evolution all the time due to invariable and non-zero rotation rate h around the x -axis, as long as the gate time is chosen appropriately, these idle qubits will evolve exactly to their original status when the operations on the qubit of interest is completed. In other words, this period of free evolution is equivalent to identity gates acting on the idle qubits. For any two adjacent qubits, there always exists one qubit with no pulse acting on at any time, leaving them be free from the annoying coupling. With this principle, operations on adjacent qubits will be made alternately. Fig. 4(b) outlines an example which allows individual arbitrary rotation operations $U_0 \otimes U_1 \otimes U_2$ on three adjacent qubits, subscript $i = 0, 1, 2$ referring to the corresponding qubit acted on. The red blocks “ g_I ” refer

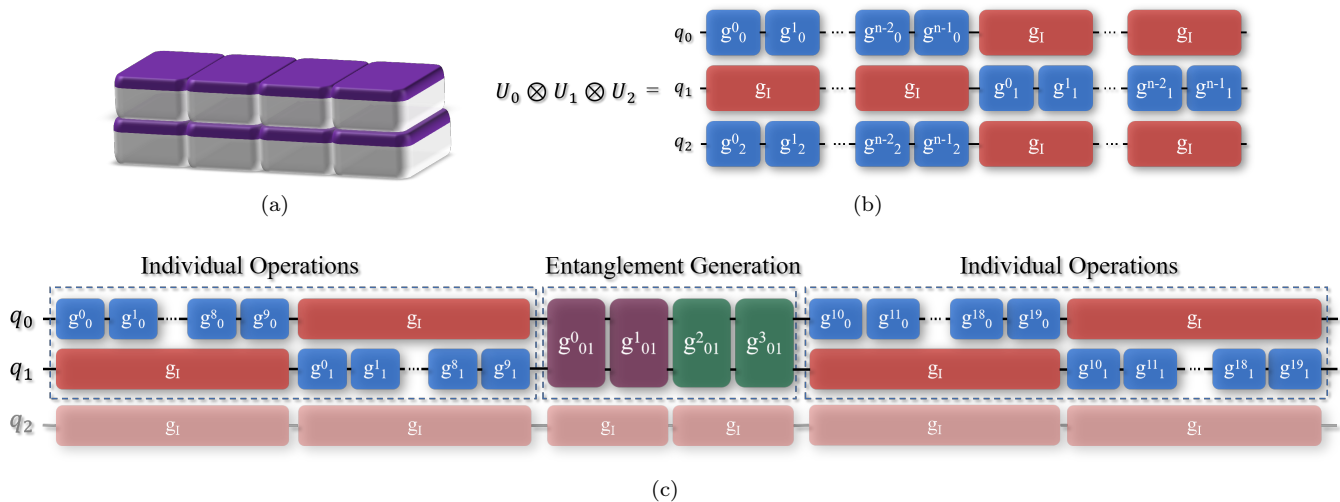


FIG. 4: (a) The vertically stacked mahjong cards which inspires us to explore the MS compilation. (b) Schematic diagram of the compiling architecture formed according to the MS compilation that enables interference-free control between qubits. (c) An Ansatz constructed in accordance with the MS compilation which enables two-qubit entangling gates acted on q_0 and q_1 , whose adjacent qubits, e.g., the q_2 , remain idle during this phase to avoid excrement interactions. The Ansatz contains three parts: two Individual Operations and one Entanglement Generation, which consist of only single-parameter native gates.

to identity gates, resulted by zero-strength pulses with $k\pi$ duration, where k is an integer (as explained in Eq. (2)). The duration of g_I here is selected twice the typical pulse time (the duration of a parametric native gate, or blue block) for clarity. This architecture possess profound implication - the allowed theme programs holded on this platform will be no longer only the precise execution of quantum gates but also the meaningful implementation of quantum algorithms.

To create two-qubit entangling gates in DQDs, e.g., CX and CZ, we likewise design empirically an Ansatz form schematically visualized in Fig. 4(c), where the entangling gate acts on q_0 and q_1 , while other adjacent qubits, e.g., the q_2 , are left idle to avert interference generation. This entanglement gate consists of three parts: one Entanglement Generation sandwiched between two Individual Operations. The part of Entanglement Generation consists of 4 sequential native

2-qubit gates (cross-qubit purple and green blocks) for generating enough entanglement between two interested qubits. Considering the fact that a two-qubit native gate is brought about by two simultaneous pulses, which impose challenge in optimization by VQA, we fix one of them to be 1 and leave the other variable. For the first two two-qubit native gates (purple blocks) we fix their parameter on q_0 , while the last two (green blocks) on q_1 . The two Individual Operations parts located before and after the Entanglement Generation are used to apply additional rotations to each qubit to achieve fine tuning for improved entire performance.

Data and code availability

The code and data that support this work are available in the online repository [65].

[1] M. A. Nielsen and I. L. Chuang, *Quantum Computation and Quantum Information 10th Anniversary Edition* (Cambridge University Press, 2010).
 [2] B. Bishnoi, [Quantum computation](https://arxiv.org/abs/2006.02799) (2021), [arXiv:2006.02799 \[quant-ph\]](https://arxiv.org/abs/2006.02799).
 [3] D. Leibfried, R. Blatt, C. Monroe, and D. Wineland, *Reviews of Modern Physics* **75**, 281 (2003).
 [4] M. Lewenstein, A. Sanpera, V. Ahufinger, B. Damski, A. Sen, and U. Sen, *Advances in Physics* **56**, 243 (2007).
 [5] M. G. Dutt, L. Childress, L. Jiang, E. Togan, J. Maze, F. Jelezko, A. Zibrov, P. Hemmer, and M. Lukin, *Science* **316**, 1312 (2007).
 [6] M. Gong, S. Wang, C. Zha, M.-C. Chen, H.-L. Huang,

Y. Wu, Q. Zhu, Y. Zhao, S. Li, S. Guo, *et al.*, *Science* **372**, 948 (2021).
 [7] Y. Wu, W.-S. Bao, S. Cao, F. Chen, M.-C. Chen, X. Chen, T.-H. Chung, H. Deng, Y. Du, D. Fan, M. Gong, C. Guo, C. Guo, S. Guo, L. Han, L. Hong, H.-L. Huang, Y.-H. Huo, L. Li, N. Li, S. Li, Y. Li, F. Liang, C. Lin, J. Lin, H. Qian, D. Qiao, H. Rong, H. Su, L. Sun, L. Wang, S. Wang, D. Wu, Y. Xu, K. Yan, W. Yang, Y. Yang, Y. Ye, J. Yin, C. Ying, J. Yu, C. Zha, C. Zhang, H. Zhang, K. Zhang, Y. Zhang, H. Zhao, Y. Zhao, L. Zhou, Q. Zhu, C.-Y. Lu, C.-Z. Peng, X. Zhu, and J.-W. Pan, *Phys. Rev. Lett.* **127**, 180501 (2021).
 [8] Q. Zhu, S. Cao, F. Chen, M.-C. Chen, X. Chen, T.-H.

- Chung, H. Deng, Y. Du, D. Fan, M. Gong, C. Guo, C. Guo, S. Guo, L. Han, L. Hong, H.-L. Huang, Y.-H. Huo, L. Li, N. Li, S. Li, Y. Li, F. Liang, C. Lin, J. Lin, H. Qian, D. Qiao, H. Rong, H. Su, L. Sun, L. Wang, S. Wang, D. Wu, Y. Wu, Y. Xu, K. Yan, W. Yang, Y. Yang, Y. Ye, J. Yin, C. Ying, J. Yu, C. Zha, C. Zhang, H. Zhang, K. Zhang, Y. Zhang, H. Zhao, Y. Zhao, L. Zhou, C.-Y. Lu, C.-Z. Peng, X. Zhu, and J.-W. Pan, *Science Bulletin* **67**, 240 (2022).
- [9] H.-L. Huang, D. Wu, D. Fan, and X. Zhu, *Science China Information Sciences* **63**, 1 (2020).
- [10] H.-S. Zhong, H. Wang, Y.-H. Deng, M.-C. Chen, L.-C. Peng, Y.-H. Luo, J. Qin, D. Wu, X. Ding, Y. Hu, and et al., *Science* **370**, 10.1126/science.abe8770 (2020).
- [11] H.-S. Zhong, Y.-H. Deng, J. Qin, H. Wang, M.-C. Chen, L.-C. Peng, Y.-H. Luo, D. Wu, S.-Q. Gong, H. Su, and et al., *Physical Review Letters* **127**, 10.1103/physrevlett.127.180502 (2021).
- [12] X. Zhang, H.-O. Li, G. Cao, M. Xiao, G.-C. Guo, and G.-P. Guo, *National Science Review* **6**, 32 (2019).
- [13] L. Vandersypen and M. A. Eriksson, *Physics Today* **72**, 38 (2019).
- [14] J. P. Dodson, N. Holman, B. Thorgrimsson, S. F. Neyens, E. R. MacQuarrie, T. McJunkin, R. H. Foote, L. F. Edge, S. N. Coppersmith, and M. A. Eriksson, *Nanotechnology* **31**, 505001 (2020).
- [15] I. Hansen, A. E. Seedhouse, K. W. Chan, F. E. Hudson, K. M. Itoh, A. Laucht, A. Saraiva, C. H. Yang, and A. S. Dzurak, *Applied Physics Reviews* **9**, 031409 (2022), <https://doi.org/10.1063/5.0096467>.
- [16] G. P. Stephan, T. M. Mateusz, V. A. Sergey, L. d. S. Sander, R. Maximilian, and K. Nima, arXiv preprint arXiv:2202.09252 (2022).
- [17] K. Takeda, A. Noiri, T. Nakajima, T. Kobayashi, and S. Tarucha, *Nature* **608**, 682 (2022).
- [18] B. M. Maune, M. G. Borselli, B. Huang, T. D. Ladd, P. W. Deelman, K. S. Holabird, A. A. Kiselev, I. Alvarado-Rodriguez, R. S. Ross, and A. E. Schmitz, *Nature* **481**, 344 (2012).
- [19] J. R. Petta, *Science* **309**, 2180 (2005).
- [20] F. K. Malinowski, F. Martins, P. D. Nissen, E. Barnes, L. Cywiński, M. S. Rudner, S. Fallahi, G. C. Gardner, M. J. Manfra, C. M. Marcus, et al., *Nature nanotechnology* **12**, 16 (2017).
- [21] D. M. Zajac, A. J. Sigillito, M. Russ, F. Borjans, J. M. Taylor, G. Burkard, and J. R. Petta, *Science* **359**, 439 (2018).
- [22] E. A. Laird, J. M. Taylor, D. P. DiVincenzo, C. M. Marcus, M. P. Hanson, and A. C. Gossard, *Phys. Rev. B* **82**, 075403 (2010).
- [23] J. Medford, J. Beil, J. M. Taylor, S. D. Bartlett, A. C. Doherty, E. I. Rashba, D. P. DiVincenzo, H. Lu, A. C. Gossard, and C. M. Marcus, *Nature Nanotechnology* **8**, 654 (2013).
- [24] Z. Shi, C. B. Simmons, J. R. Prance, J. K. Gamble, and S. N. Coppersmith, *Physical Review Letters* **108**, 140503 (2012).
- [25] D. Kim, Z. Shi, C. B. Simmons, D. R. Ward, J. R. Prance, T. S. Koh, J. K. Gamble, D. E. Savage, M. G. Lagally, and M. a. Friesen, *Nature* (2014).
- [26] H. Bluhm, S. Foletti, D. Mahalu, V. Umansky, and A. Yacoby, *APS*, P17 (2009).
- [27] F. T. Chong, D. Franklin, and M. Martonosi, *Nature* **549**, 180 (2017).
- [28] A. Paler, I. Polian, K. Nemoto, and S. J. Devitt, *Quantum Science and Technology* **2**, 025003 (2017).
- [29] A. W. Cross, L. S. Bishop, J. A. Smolin, and J. M. Gambetta, arXiv preprint arXiv:1707.03429 (2017).
- [30] R.-H. He, R.-F. Hua, A. Ablimit, and Z.-M. Wang, arXiv preprint arXiv:2204.02555 (2022).
- [31] X.-M. Zhang, Z. Wei, R. Asad, X.-C. Yang, and X. Wang, *npj Quantum Information* **5**, 1 (2019).
- [32] X. Wang, L. S. Bishop, E. Barnes, J. Kestner, and S. D. Sarma, *Physical Review A* **89**, 022310 (2014).
- [33] X. Wang, L. S. Bishop, J. Kestner, E. Barnes, K. Sun, and S. Das Sarma, *Nature communications* **3**, 1 (2012).
- [34] J. P. Kestner, X. Wang, L. S. Bishop, E. Barnes, and S. D. Sarma, *Physical review letters* **110**, 140502 (2013).
- [35] M.-Y. Chen, C. Zhang, and Z.-Y. Xue, *Physical Review A* **105**, 022620 (2022).
- [36] X.-C. Yang, M.-H. Yung, and X. Wang, *Physical Review A* **97**, 042324 (2018).
- [37] I. Goodfellow, Y. Bengio, and A. Courville, *Deep Learning* (The MIT Press, USA, 2016).
- [38] R.-H. He, R. Wang, J. Wu, S.-S. Nie, J.-H. Zhang, and Z.-M. Wang, *Deep reinforcement learning for universal quantum state preparation via dynamic pulse control* (2021).
- [39] Y.-H. Zhang, P.-L. Zheng, Y. Zhang, and D.-L. Deng, *Physical Review Letters* **125**, 170501 (2020).
- [40] T. Haug, W.-K. Mok, J.-B. You, W. Zhang, C. E. Png, and L.-C. Kwek, *Machine Learning: Science and Technology* **2**, 01LT02 (2020).
- [41] R.-H. He, H.-D. Liu, S.-B. Wang, J. Wu, S.-S. Nie, and Z.-M. Wang, *Quantum Science and Technology* **6**, 045021 (2021).
- [42] C. Ferrie, *Physical review letters* **113**, 190404 (2014).
- [43] M. Broughton, G. Verdon, T. McCourt, A. J. Martinez, J. H. Yoo, S. V. Isakov, P. Massey, R. Halavati, M. Y. Niu, A. Zlokapa, et al., arXiv preprint arXiv:2003.02989 (2020).
- [44] M. Benedetti, E. Lloyd, S. Sack, and M. Fiorentini, *Quantum Science and Technology* **4**, 043001 (2019).
- [45] P. Rakyta and Z. Zimborás, *Quantum* **6**, 710 (2022).
- [46] P. Rakyta and Z. Zimborás, arXiv preprint arXiv:2203.04426 (2022).
- [47] R. Chen, B. Zhao, and X. Wang, arXiv preprint arXiv:2109.10785 (2021).
- [48] X.-Z. Luo, J.-G. Liu, P. Zhang, and L. Wang, *Quantum* **4**, 341 (2020).
- [49] L. K. Grover, in *Proceedings of the twenty-eighth annual ACM symposium on Theory of computing* (1996) pp. 212–219.
- [50] G. Brassard, P. Hoyer, M. Mosca, and A. Tapp, *Contemporary Mathematics* **305**, 53 (2002).
- [51] G.-L. Long, *Physical Review A* **64**, 022307 (2001).
- [52] L. P. Taylor, K. Jean, A. Anima, and F. Y. Susanne, arXiv preprint arXiv:2106.13304v4 (2022).
- [53] M. P. Harrigan, K. J. Sung, M. Neeley, K. J. Satzinger, F. Arute, K. Arya, J. Atalaya, J. C. Bardin, R. Barends, S. Boixo, et al., *Nature Physics* **17**, 332 (2021).
- [54] A. Peruzzo, J. McClean, P. Shadbolt, M.-H. Yung, X.-Q. Zhou, P. J. Love, A. Aspuru-Guzik, and J. L. O'Brien, *Nature communications* **5**, 1 (2014).
- [55] G. A. Quantum, Collaborators, F. Arute, K. Arya, R. Babbush, D. Bacon, J. C. Bardin, R. Barends, S. Boixo, M. Broughton, B. B. Buckley, et al., *Science* **369**, 1084 (2020).

- [56] S. Stanisic, J. L. Bosse, F. M. Gambetta, R. A. Santos, W. Mruzckiewicz, T. E. O'Brien, E. Ostby, and A. Montanaro, arXiv preprint arXiv:2112.02025 (2021).
- [57] C. W. Commander, *Encyclopedia of Optimization* **2** (2009).
- [58] J. Preskill, *Quantum* **2**, 79 (2018).
- [59] W. Jang, M.-K. Cho, J. Kim, H. Chung, V. Umansky, and D. Kim, *Applied Physics Letters* **117**, 234001 (2020).
- [60] X. Wu, D. R. Ward, J. Prance, D. Kim, J. K. Gamble, R. Mohr, Z. Shi, D. Savage, M. Lagally, M. Friesen, *et al.*, *Proceedings of the National Academy of Sciences* **111**, 11938 (2014).
- [61] M. D. Shulman, O. E. Dial, S. P. Harvey, H. Bluhm, V. Umansky, and A. Yacoby, *Science* **336**, 202 (2012).
- [62] J. M. Nichol, L. A. Orona, S. P. Harvey, S. Fallahi, G. C. Gardner, M. J. Manfra, and A. Yacoby, *npj Quantum Information* **3**, 1 (2017).
- [63] P. K. Diederik and B. Jimmy, arXiv preprint arXiv:1412.6980v9 (2017).
- [64] S. McArdle, S. Endo, A. Aspuru-Guzik, S. C. Benjamin, and X. Yuan, *Reviews of Modern Physics* **92**, 015003 (2020).
- [65] R.-H. He, *Code and data supported this paper* (2022).
- [66] W. Li, Y. Ding, Y. Yang, R. S. Sherratt, J. H. Park, and J. Wang, *Human-centric Computing and Information Sciences* **10**, 1 (2020).
- [67] J. Preskill, arXiv preprint arXiv:1203.5813 (2012).
- [68] A. Lucas, *Frontiers in physics* , 5 (2014).
- [69] E. Farhi, J. Goldstone, and S. Gutmann, arXiv preprint arXiv:1411.4028 (2014).
- [70] M. Fishman, S. White, and E. Stoudenmire, *SciPost Physics Codebases* , 004 (2022).
- [71] J. C. Bridgeman and C. T. Chubb, *Journal of physics A: Mathematical and theoretical* **50**, 223001 (2017).
- [72] W. Huggins, P. Patil, B. Mitchell, K. B. Whaley, and E. M. Stoudenmire, *Quantum Science and technology* **4**, 024001 (2019).
- [73] M. Developer, *Mindquantum, version 0.6.0* (2021).
- [74] D. C. McKay, C. J. Wood, S. Sheldon, J. M. Chow, and J. M. Gambetta, *Physical Review A* **96**, 022330 (2017).
- [75] V. V. Shende, I. L. Markov, and S. S. Bullock, *Physical Review A* **69**, 062321 (2004).
- [76] E. Farhi and H. Neven, arXiv preprint arXiv:1802.06002 (2018).
- [77] R. Sweke, F. Wilde, J. Meyer, M. Schuld, P. K. Fährmann, B. Meynard-Piganeau, and J. Eisert, *Quantum* **4**, 314 (2020).
- [78] A. W. Harrow and J. C. Napp, *Physical Review Letters* **126**, 140502 (2021).
- [79] Y.-Y. Xie, F.-H. Ren, R.-H. He, A. Ablimit, and Z.-M. Wang, arXiv preprint arXiv:2208.08261 (2022).

Acknowledgment

This work was supported by the Natural Science Foundation of Shandong Province (Grant No. ZR2021LLZ004), and the Natural Science Foundation of China (Grant No. 11475160). The author RHH would also like to thank Shang-Shang Shi and Guo-Long Cui personally for fruitful discussions.

Author contributions

ZM Wang, XS Xu and RH He established the key idea in this paper. RH He did the numerical experiments and wrote the draft paper under the guidance of ZM Wang and XS Xu. All the authors contributed to the preparation of this paper.

Competing interests

The authors declare no competing interests.

Correspondence should be addressed to ZM Wang or XS Xu.